Kinematic analysis of bimanual movements during food handling by head-fixed rats

Masakazu Igarashi and Jeff Wickens

Neurobiology Research Unit, Okinawa Institute of Science and Technology Graduate University, Okinawa, Japan

Running Head

Kinematic analysis of bimanual movements in rats

Author contributions

M.I. and J.W. designed experiments. M.I. conducted experiments and drafted manuscript and figures. J.W. revised manuscript.

Corresponding author

Jeff Wickens or Masakazu Igarashi

Neurobiology Research Unit, Okinawa Institute of Science & Technology Graduate University

1919-1 Tancha, Onna, Okinawa, 904-0495, Japan

ABSTRACT

Bimanual coordination – in which both hands work together to achieve a goal – is crucial for the basic needs of life, such as gathering and feeding. Such coordinated motor skill is highly developed in primates, where it has been most extensively studied. Rodents also exhibit remarkable dexterity and coordination of forelimbs during food handling and consumption. However, rodents have been less commonly used in the study of bimanual coordination because of limited quantitative measuring techniques. Here we describe a high-resolution tracking system that enables kinematic analysis of rat forelimb movement. The system is used to quantify forelimb movements bilaterally in head-fixed rats during food handling and consumption. Forelimb movements occurring naturally during feeding were encoded as continuous 3-D trajectories. The trajectories were then automatically segmented and analyzed, using a novel algorithm, according to the laterality of movement speed or the asymmetry of movement direction across the forelimbs. Bilateral forelimb movements were frequently observed during spontaneous food handling. Both symmetry and asymmetry in movement direction were frequently observed, with symmetric bilateral movements quantitatively more common. The proposed method overcomes a limitation in the precise quantification of bimanual coordination in rodents. This enables the use of powerful rodent-based research tools such as optogenetics and chemogenetics in the further investigation of neural mechanisms of bimanual coordination.

Keywords

bimanual coordination; head-fixed; motion capture technology; classification of behavior; kinematic analysis.

New & Noteworthy

We describe a new method for quantifying and classifying three-dimensional, bilateral forelimb trajectories in head-fixed rats. The method overcomes limits on quantifying bimanual coordination in rats. When applied to kinematic analysis of food handling behavior, cdontinuous forelimb trajectories were automatically segmented and classified. Bilateral forelimb movements were observed more frequently than unilateral movements during spontaneous food handling. Both symmetry and asymmetry in movement direction were frequently observed. However, symmetric bilateral forelimb movements were more common.

INTRODUCTION

The ability to execute bimanual actions –involving the coordinated interplay of both limbs – is crucial not only for the most basic needs of daily life, such as gathering and feeding, but also for the heights of human creative achievement exhibited in art and music. Despite being computationally expensive, the ability to coordinate the limbs bilaterally has been advantageous and selected for in evolution. The neural mechanisms underlying bimanual movements have long been a focus of research in primates because of their significance for behavioral neuroscience, for the pathophysiology of movement disorders, and as a basis for rehabilitation or diagnosis (Ponsen et al. 2006; Reinkensmeyer et al. 2016; Swinnen 2002; Swinnen and Wenderoth 2004; van Delden et al. 2012; Wu et al. 2010). Many important advances toward understanding bimanual coordination have been made using human and non-human primates as the experimental subject (Swinnen 2002). Primates have many advantages because of their advanced capabilities and the availability of sophisticated analytical apparatus. However, primates are less well suited to invasive experimental manipulations, or the use of transgenic approaches to understand the neural mechanisms. In contrast, such manipulations are readily applied in rodent models, which are therefore advantageous for addressing neural mechanisms of the mammalian brain. Like primates, rodents also exhibit dexterous coordination of forelimbs to handle food objects when eating (Whishaw and Coles 1996). There is, therefore, much to be gained from further developing quantitative and qualitative measuring techniques suitable for use with rodent models in the study of bimanual coordination. The aim of the present investigation was to develop a method for quantifying bimanual movement in the rat.

Quantification of bimanual coordination during spontaneous food handling behavior has been reported in freely moving (Allred et al. 2008; Tennant et al. 2010; Whishaw and Coles 1996) and head-fixed rodents (Whishaw et al. 2017b). Evaluation of behavior in these reports has been based on investigator observation of action and postures of hands by off-line video analysis. In recent years, the emergence of kinematic analysis with 2-D lever and 3-D motion capture has enabled the documentation of qualitative measures such as tortuosity, oscillations, and variability in unimanual

73 motor control (Azim et al. 2014; Guo et al. 2015; Kawai et al. 2015; Palmér et al. 2012; Panigrahi et
74 al. 2015). Implementation of these analytical techniques has furthered our fundamental
75 understanding of rodent motor behavior. However, it is important to extend these methods to the
76 problems of classification of bimanual movements during natural action sequences.

77 Here we report an imaging system for measuring bimanual coordination in rats. The system
78 uses a pair of high-speed cameras to capture 3-D forelimb position during bimanual food handling.
79 In the system, rats are head-fixed in order to provide a reference frame for recording. A semi-
80 automated tracking program generates trajectories of forelimb position in animal egocentric 3-D
81 space. Trajectories are transformed into kinematic parameters such as speed, velocity, or movement
82 direction. To show potential uses of kinematic data obtained with the system, we demonstrate
83 segmentation and mathematical analysis of rat forelimb movements to measure laterality of
84 movement speed and asymmetry of movement direction during food handling. Finally, using a
85 classification algorithm, we demonstrate high-throughput of large amount of kinematic data from
86 multiple rats to quantify spontaneous food handling behavior.

MATERIALS AND METHODS

Animals. Ten- to twelve-week-old Male Long Evan rats weighing 350-450 g were kept under a reversed 12 hrs light/dark cycle (10:00 am to 10:00 pm), constant temperature (25°C) and humidity. Rats were housed with *ad libitum* access to water and food before weight restriction. Animals were habituated to the experimenter for more than three days before the start of behavioral recording. All experiments were approved by the Committee for Care and Use of Animals at the Okinawa Institute of Science and Technology.

Surgery for head-fixation. Carprofen (Rimadyl, Pfizer, 50 mg ml^{-1}, sc) was administered immediately before surgery. Rats were anesthetized with isoflurane (3 - 4% induction, 1.5 - 2.5 % for maintenance), and placed on a stereotaxic frame for chronic experiments (SR-10R-HT, Narishige, Japan). Body temperature was monitored and maintained at 36.5 - 37.5ºC with a heating pad. The skull was exposed and carefully cleaned with saline and cotton swabs. Super-Bond Green Activator (Sun Medical Inc., Japan) was judiciously applied to the skull, left for 20 sec, and then removed by saline. After the surface preparation, eight anchor screws (M 1 × 2) were drilled into the skull. The screws were then covered with a layer of dental cement (Super-Bond, Sun Medical Inc., Japan). A chamber frame (CFR-1, Narishige, Japan) was positioned above the skull and secured by additional layers of dental cement. Antibiotic was intraperitoneally administered after the surgery. A dietary supplement with Carprofen (Medigel CPF; Clear H_2O, ME., US.) was given during post-op recovery for 5 days.

Behavioral apparatus and recording setup. A custom made stereotaxic frame for chronic experiments (SR-10R-HT, Narishige, Japan) was used for head-fixed behavioral experiments. A 3-D printed passive linear treadmill (80 mm wide and 130 mm long; Fig. 1A) was used to minimize animals' stress by allowing hindlimb movement. The treadmill was placed above a transparent acrylic base plate, and two high-speed cameras (HAS-L1, f = 6mm, DITECT, Japan) with infrared

LEDs were positioned 45 cm below the base to monitor forelimbs (Fig. 1 B and C). The two cameras were placed 130 mm apart and directed at an angle of 30° to each other. The accuracy of depth reconstruction was confirmed by using the MATLAB Stereo Camera Calibrator application. The mean reprojection error (the mean distance between the detected marker position and the reprojected points in the reconstructed model space) was 0.77 pixels (Hartley and Zisserman 2003).

Habituation to head-fixation and pre-training. Rats were food restricted prior to behavioral training. Body weight was maintained between 80 % and 90 % of the original weight. Animals were then habituated to the head-fixed apparatus. Habituation was based on the procedures previously reported (Isomura et al. 2009; Ollerenshaw et al. 2012; Schwarz et al. 2010), but modified for food restriction. Briefly, rats underwent the following steps: (1) Rats were placed in the behavioral chamber with *ad libitum* access to food for 20 min for 2 days. (2) The experimenter guided the rats into the half-cylindrical tunnel by providing a sweet jelly reward (Purin mix, House foods, Japan) using a stainless reward spout connected to a 50 mL syringe. The experimenter controlled the position of reward spout to induce animals to slide the chamber frame into the head attachment clamp. 10 – 20 ml of reward was provided in a day. (3) The experimenter held the rat's chamber with gentle force while providing reward. Initially, some rats tried to escape, and it took 2 - 3 attempts for the rats to retrieve 10 - 20 ml of sweet jelly reward. (4) Pre-training. Immediately after head-fixation, the experimenter gave a food reward cut into an annular shape (20 mm outer diameter, 10 mm inner diameter, 5 mm thickness, Fish Sausage, Marudai Food Co., Ltd, Japan) instead of the jelly reward. The pre-training continued until rats could retrieve, without dropping, five rewards for three consecutive days.

Behavioral task and recording. The reflective markers were handmade by covering a 3 mm diameter plastic half sphere with reflective tape (DITECT, Japan). On the day of the behavioral task, the experimenter gently held the forelimbs while the half-spherical markers were attached to the

lower side of the wrists using double-sided tape. The marker could be removed easily after behavioral testing. Rats did not try to remove the marker during the behavioral task. Trials started with bimanual grasping of food offered by the experimenter (Fig. 1E), and ended when the last piece of food was brought to the mouth. Rats underwent 16 - 21 trials in three days (5 - 7 trials per a day). Cases where rats showed unusual behavior, such as crossing two forelimbs or adopting a tripedal stance during eating, were excluded from further analysis. In the present study, only two cases out of 79 recorded session across five rats were excluded. All trials were recorded at 200 frames per second (1/500s exposure time and 600x800 pixel) and stored to hard disk.

High-speed cameras and 3-D reconstruction. The positions of reflective markers were traced using an in-house program assembled from a MATLAB toolbox (Computer Vision System Toolbox release 2016b, The MathWorks, Inc., MA., USA). Tracking was automatic except for adjustments to tracking parameters such as threshold which were required in response to the changes in reflection caused by marker angle. The program produced *x* and *y* coordinates of the marker position from 2-D video frames of Camera #1 and Camera #2. Depth reconstruction of the marker point was estimated by triangulation of the paired points on the 2D plane from Camera #1 and Camera #2 and the camera geometries. The resulting 3-D positions of the reflective marker in the camera coordinate system were represented as a time series data $(\mathrm{x_t}, \mathrm{y_t}, \mathrm{z_t})$. Depth reconstruction of marker position and calibration of camera position were conducted using the stereo camera calibrator package of the *MATLAB Computer Vision System Toolbox*. The reference frame defining the egocentric coordinate axes was included in the field of view of the cameras (Fig. 2A, B). Using this reference, the 3-D position data (x_t, y_t, z_t) was transformed into the egocentric coordinate system (lr_t, ap_t, dv_t) which represented time series data of forelimb position in left-right (lr) axis, anterior-posterior (ap) axis, and dorsal-ventral (dv) axis (Fig. 2 C). All data were filtered through a 20-Hz low-pass finite impulse response filter.

Discretization of time series data. Continuous position data were discretized into 50 ms duration segments, s_t (Equation 1), with 5 ms shifts (Fig. 2D, E). The segment s_t was defined as the array of 3-D position data of right and left forelimbs in a 50 ms time window.

$$s_t = \begin{bmatrix} lr_t & \cdots & lr_{t+50ms} \\ ap_t & \cdots & ap_{t+50ms} \\ dv_t & \cdots & dv_{t+50ms} \end{bmatrix} \#(1)$$

All segments of the right and left forelimb, s_{Rt} and s_{Lt}, were stored as the set $S \ni \begin{bmatrix} s_{Rt} \\ s_{Lt} \end{bmatrix}_{1,2,\cdots,N}$, where s_{Rt} and s_{Lt} are vertically stacked. The sets, S, from different trials were horizontally concatenated. Therefore, the total number of segments N depend on the time of each trial and number of trials used for analysis. All segments in the set S were evaluated by classification scoring methods.

Qualitative measure of forelimb movements and classification. All segments of behavioral data were analyzed by the following three steps (Fig. 3):

(1) Extraction of moving segments. We first defined the maximum speed function $max(\bar{V}_R, \bar{V}_L)$, where $\bar{V}_R$ and $\bar{V}_L$ are mean speed in a segment s_R and s_L. The function returns the value of maximum speed among right or left forelimb in a segment. We defined the moving segment as $max(\bar{V}_R, \bar{V}_L) \geq 40\ (mm/sec)$. That is, if mean speed of either left or right forelimb exceeded a threshold, the segment was classified as a moving segment. Conversely, resting segments were defined as $max(\bar{V}_R, \bar{V}_L) < 40\ (mm/sec)$. The all moving segments were then analyzed by following two metrics: (2) Speed Ratio, and (3) Asymmetry index.

(2) Speed Ratio Function. Bilateral forelimb movement was considered to occur when

movement amplitude across limbs remained uniform within a set limit; conversely, unilateral forelimb movement was considered to occur when there was significantly biased movement amplitude across limbs. To formalize the definition of bilateral and unilateral forelimb movement, the speed ratio of forelimbs was used (Equation 2).

$$SpeedRatio = \frac{\min\{\bar{V}_R, \bar{V}_L\}}{\max\{\bar{V}_R, \bar{V}_L\}} \#(2)$$

The *SpeedRatio* function is a measure of laterality of speed across both forelimbs, where 1 indicates equal movement amplitude across the two forelimbs.

Movements were classified as bilateral or unilateral. A criterion of $\text{SpeedRatio} \geq 0.5$ was used to isolate bilateral movements across two forelimbs, indicating when one forelimb was moving at no more than twice the speed of the other forelimb. Conversely, $\text{SpeedRatio} < 0.5$ was used to define unilateral movements, indicating when one forelimb moved at least twice as fast as the other forelimb in that segment. The boundary value was set to the half-maximum of SpeedRatio which is 0.5.

(3) Asymmetry index. Symmetric movements are also called mirror movements in cases where one limb moves as a mirrored copy of the contralateral limb. Physiologically, symmetry implies synchronized activation of homologous muscle groups, and asymmetry implies activation of non-homologous muscle groups. This definition is embedded in the egocentric framework discussed by Swinnen et al. (1998, 2001), in which movement is related to the longitudinal axis of the body and the coordination of corresponding limbs. The alternative, allocentric framework was not used in the present study because the limb movements were referenced to the body rather than the surrounding space. We defined symmetric movements as movement in the similar movement direction by both forelimb. Conversely, asymmetry index θ (Equation 3), is the angle

between movement direction of the velocity vector of the left forelimb v_L (Equation 4) and the mirror transformed velocity vector of right forelimb v_{R_M} (Equation 5), estimated by the inverse cosine similarity function.

$$\theta = cos^{-1}\left(\frac{v_{R\_M} \cdot v_L}{|v_{R\_M}||v_L|}\right) \#(3)$$

$$v_L = \left(\frac{\Delta lr_L}{\Delta t}, \frac{\Delta ap_L}{\Delta t}, \frac{\Delta dv_L}{\Delta t}\right) \#(4)$$

$$v_{R\_M} = \left(-\frac{\Delta lr_R}{\Delta t}, \frac{\Delta ap_R}{\Delta t}, \frac{\Delta dv_R}{\Delta t}\right) \#(5)$$

The mean asymmetry index of a segment $\bar{\theta}$ was calculated from the mean of θ in a 50 ms time window.

With the estimated $\bar{\theta}$, symmetric and asymmetric movements were classified. A segment was defined as symmetric movement if $\bar{\theta} < \pi/4$ where the angle of movement direction of the left forelimb and mirrored right forelimb remained less than 45 degrees. Conversely, a segment was defined as asymmetric movement if $\bar{\theta} \geq \pi/4$, indicating that the angle between the two velocity vectors was greater than or equal to 45 degrees (Fig.3). The boundary value was based on the previous literature in which orthogonal lever press of two hands was defined as asymmetric bimanual movement (Cardoso de Oliveira et al. 2001). The present study used the value $\pi/4$ which is intermediate between perfect symmetric movement (0 degrees) and orthogonal asymmetric movements (90 degrees).

RESULTS

Behavior in the apparatus during training. After habituation to head-fixation, all rats spontaneously entered the treadmill. Some rats were able to slide the chamber frame into the head attachment clamp without the experimenter's guidance. All rats were able to perform food handling while in the head-fixed position. The rats rarely dropped food during bimanual food handling, showing a mean success rate (food consumption without dropping) of 97.89 ± 2.90%, and a mean consumption time of 27.92 ± 2.77 sec per trial (n = 5). Overall, head-fixation did not impede spontaneous food manipulation.

During food consumption, rats made periodic transitions between resting and moving. In the resting state, rats held the food item in a low position, and chewed on it. During movement, rats brought the food item to a higher position and dynamically manipulated it, changing the holding position and rotating the object. Frequently observed behaviors are shown in single video frames in Fig. 4A-D. Some of these behaviors have been reported by Whishaw and colleagues (Whishaw and Coles 1996; Whishaw et al. 2017b). Rats exhibited bimanual downward and upward reaching behaviors at different times. On first exposure to the food item, reaching down, grasping, and upward movement of the forelimbs occurred to bring the food item toward and against the mouth. These movements often punctuated the transition between resting and active states. In some cases, rats used the downward reaching behaviour to break the food item by tearing with the teeth. The bimanual and unimanual displacements involved in releasing and holding the food item were usually seen when rats changed their grasping position (Fig. 4C, D).

To interpret the 3-D trajectories of typical forelimb actions, we compared the video frames of representative manually identified behaviors with the corresponding 3-D scatter plots of wrist position marker coordinates (Fig. 4, right column). We found that the sequence of wrist positions as represented in the scatter plots clearly illustrated bimanual and unimanual behaviors. For example, upward bimanual reach was evident in the sequence of points indicating the position of each wrist as

they shifted towards the ventral side (Fig. 4A). In unimanual movements the separation between the points corresponding to the moving wrist indicated larger displacements, contrasting with the closely spaced points corresponding to the other, relatively stationary forelimb (Fig. 4D). These observations illustrate the potential of analyzing the transition of wrist positions for quantifying several types of active forelimb states.

Full 3-D reconstruction of position of wrists. To provide a basic data set of the entire action sequence of an eating behavior, time series data of wrist positions in egocentric coordinates were generated from 77 trials across 5 rats. Representative trajectories of both wrists in the egocentric coordinate space are shown in Fig. 5. On the ventral side, forelimbs followed an arc-shaped relatively convergent trajectory, whereas on the dorsal side the trajectories diverged and became intermingled. The intermingled structure suggests that food manipulation consists of highly variable action patterns, such as symmetric/asymmetric bimanual movements and unimanual movements. To categorize forelimb use during continuous action sequences, we segmented the continuous time series data of wrist positions using a 50 ms sliding time window (Fig. 2D, E). The segments were generated from all data sets across 5 rats, and subjected to analysis in order to score and classify them into subtypes of unimanual and bimanual movements.

Extraction of Moving segments. We considered movement to be occurring whenever the speed of one limb exceeded a threshold of 40 mm/sec (Fig. 6A-E). This non-zero criterion for "movement" was chosen because, even in the resting state, some physiological activity such as chewing, breathing, or sniffing, causes jittering of the forelimb position. The probability distribution of forelimbs speed showed a natural dip around 40mm/sec (Fig. 6A). The natural dip was also seen in the probability distribution of the processed speed variable which is maximum speed function (Fig. 6B). Thus, the thresholding process removed physiological movement artefacts. According to this criterion the portion of time spent moving was 0.29 ± 0.05 (Fig. 6C, $n = 5$).

Bilateral movements vs unilateral movements. The extracted moving segments described above included both bilateral and unilateral forelimb movements. We analyzed these movements, based on the laterality of movement speed across two forelimbs by applying the speed ratio function (Fig. 7). The speed ratio was defined as the ratio of mean speeds between two forelimbs in a segment, based on the idea that both forelimbs move at similar amplitude for bilateral movements, while one forelimb moves faster than the other in unilateral movements (Fig. 7A-B). We found that the mean probability distribution of the speed ratio was biased towards 1, suggesting that the majority of forelimb movements during food handling were bilateral; conversely, unilateral forelimb movements were less frequent (Fig. 7B). Some representative segments of bilateral or unilateral forelimb movements based on the boundary value of 0.5 are shown in Fig. 7C, D.

Symmetric vs asymmetric movement. One of the main purposes of the kinematic analysis of forelimb movements is to determine the relative amounts of symmetric and asymmetric movement during the natural sequence of food handling behavior (Fig 8A-D). Symmetric bimanual movements are a subset of bimanual movements generated by the activation of homologous muscle groups across two limbs. Conversely, an asymmetric bimanual movement is caused by different (non-homologous) muscle groups. In the present study, symmetric bimanual movements were defined as those in which the movement direction of a forelimb mirrors the other forelimb with respect to the sagittal plane of the body (Fig. 8A). The asymmetry index θ is found by subtracting the angle of movement direction of a forelimb from the mirrored angle of the contralateral forelimb movement.

We assigned the asymmetry index θ to each segment, and calculated the probability density function of the asymmetry index. The probability distribution was significantly biased in the less asymmetric direction suggesting that the symmetric state predominates (Fig. 8B). Representative symmetric or asymmetric movements based on the boundary value of $\pi/4$ are shown in Fig. 8C, D.

310

311 *High-throughput analysis of kinematic data for quantification of forelimb movements.* Finally,
312 many (more than 430,000) segments from 77 trials across 5 rats were subjected to automatic analysis
313 and classification. The speed ratio and asymmetry index of all moving segments were measured (Fig.
314 9). The classification algorithm (Fig. 3) was applied to all segments to illustrate the time series of the
315 following motor behaviors: bilateral movement, unilateral movement, symmetric movement, or
316 asymmetric movement. The time series data of those categories of motor behavior revealed the
317 frequent transition of movement mode during feeding behavior (Fig.9A and B). The transition of
318 movement mode was visualized by overlaying the colored movement categories on the continuous
319 3D trajectories of forelimb position (Fig. 9C). The time fraction of unilateral versus bilateral and
320 symmetric versus asymmetric movements were quantified. Relative frequency of each mode of
321 forelimb movements revealed the organization of bimanual motor behavior during the natural
322 sequence of eating (Fig. 9D). The mean percentages of forelimb use in respect of movement
323 amplitude were 89% of bilateral movements and 11% of unilateral movements. The mean
324 percentages of forelimb use in respect of movement direction were 41% of asymmetric movement
325 and 59% of symmetric movement.

DISCUSSION

We report on the development of a high-resolution tracking system for kinematic analysis of rat forelimb movements and its application to the study of bimanual coordination. The system uses optical motion tracking to obtain 3-D bimanual wrist movement trajectories from natural action sequences. The 3-D trajectories were used in the kinematic analysis of coordination of forelimb movements in head-fixed rats during food handling and consumption. Movement laterality and asymmetry across forelimbs was quantified in movement segments automatically extracted from the continuous action sequence. Results showed that the speed of forelimb movement during eating behavior were highly balanced bilaterally. Symmetry in movement direction was more frequently observed than asymmetry. However, a considerable amount of asymmetry in movement direction was also observed. To our knowledge, this is the first application of this method to visualizing bilateral forelimb trajectories during spontaneous food handling behavior in rodents, extending previous studies of food handling behavior.

Limb use in spontaneous food handling behavior was first reported as a method of motor assessment in rats by Whishaw and Coles (1996). Since then, this quantitative method has been widely used to assess motor function in research on movement disorders and motor control (Allred et al. 2008; Brown and Teskey 2014; Manfré et al. 2017; Tennant et al. 2010; Wang et al. 2017; Xu et al. 2009). In these earlier studies, assessment of forelimb motor skills relied on manual identification. Grasping pattern, position of forelimb, timing of adjustment as well as global scores such as consumption time and drop rate required manual observation of video frames. The present study extends this method of assessment of motor skill in food handling behavior by using a kinematic tracking system. The sub-second kinematic information obtained from this system enables detection of subtle changes in behavior, such as changes in the ratio of symmetric to asymmetric activity during bimanual movement. Such measurements are difficult to obtain by manual observation of video frames.

Quantifying the incidence of specific motor patterns during natural action sequences is challenging. To make quantitative analysis feasible, the study of motor control often focuses on trained, repetitive, uniform action sequences such as skilled reaching, and lever pressing tasks (Guo et al. 2015; Hira et al. 2013; Isomura et al. 2009; Kawai et al. 2015; Palmér et al. 2012). Measures of such motor patterns are low dimensional, not requiring extensive data processing, unlike more natural sequences. In contrast to these more uniform action sequences, food handling behavior involves highly variable action sequences of forelimb movements. While the analysis of such sequences is more demanding, they provide good examples of naturally occurring bimanual coordination.

To quantify natural action sequences, it is necessary to identify specific behaviors when they occur. Segmentation with a sliding window, as used in the present study, is commonly used to detect behavioral events in time series data sets such as moving pictures and multi-point body kinematic information, in human as well as animal behavior (Burgos-Artizzu et al. 2012; Liu et al. 2009). Once the analytical criteria for a specific behavior – the *"detector"* – has been defined, the behavior can be identified in the continuous sequence dataset. Our mathematical definitions of bimanual movements were used to detect bilateral versus unilateral, and symmetric versus asymmetric forelimb movements within the natural action sequence data (Fig.9).

In the present study, we demonstrated the use of a movement asymmetry index and speed ratio for quantifying asymmetry of movement direction and laterality of movement speed. A limitation of this strategy is that each class of movement includes actions which may be mediated by different neuromotor channels (Whishaw et al. 2017a). For example, movements classified as symmetric bilateral forelimb movements in the present study involve movement symmetry with bimanual holding (Fig.4A) and bimanual release (Fig.4C). Specific motor behaviors such as

movement of hand to mouth, or reaching, may require a distinct movement detection algorithm. For instance, the distance between mouth position and forelimb position could be useful in defining hand to mouth movements. Another limitation is that the present movement detection has the threshold of 40mm/sec. The threshold would not permit the detection of slow bilateral forelimb movements such as the moment during transition from resting to upward reach. To study, in particular, slow upward motion arising from rest, another definition of movement onset based on position, such departure from a delineated area defined as resting position, might be useful. Recently, dimensionality reduction algorithms and machine learning approaches have captured action repertoires from natural action sequences (Berman et al. 2014; Robie et al. 2017). Further development is needed for exploring bimanual action patterns from bimanual food handling behavior.

The proposed mathematical definitions of symmetric and asymmetric bimanual movement were based on movements of the forelimb markers. Physiologically, however, symmetric versus asymmetric bimanual movements are distinguished by the pattern of activated muscle groups across limbs. For instance, simultaneous activation of homologous muscle groups generates symmetric bimanual movements. In contrast, activating different muscle groups with the same timing causes asymmetric bimanual movements. The present definition of the asymmetry, index θ, is the directional error between movement vectors of forelimbs calculated by the cosine similarity function. It is based on the idea that the activation of identical muscle groups across forelimbs results in mirror-image endpoint trajectories. This implicitly assumes that movement and muscle activity are measures of the same thing. However, it should be noted that significant physical perturbations may occur and cause, in response, changed muscle activation patterns even though the trajectory of the forelimb marker is unchanged. Thus, in the proposed system, perturbations such as bumping a part of the head-fixing device, should be excluded from the analysis.

Using the proposed system in the present study led to the finding that both asymmetric and

symmetric bilateral movements occur in food handling behavior, with symmetric bilateral forelimb movements quantitatively more commonly observed. In rodents, previous studies of forelimb use have observed laterality in grasping (a release to regrasp movements against food object) and holding position asymmetry in food handling (Allred et al. 2008; Whishaw and Coles 1996; Whishaw et al. 2017b). The present study further extended the previous results by adding that asymmetry was observed in dynamic bilateral forelimb use in rats. Our results suggest that symmetric bilateral forelimb movements were more frequently observed than asymmetric bilateral forelimb movements during handling of donut-shaped food reward. The shape of the food may have been a factor in the symmetry of the hand to mouth movements in feeding, functionally linking the forelimbs together when they were used to bring the food item to the mouth (Fig. 4A). Another possible interpretation is that the animal has natural tendency towards symmetric movements, which has been reported in various experimental conditions in humans (Swinnen 2002). Symmetric forelimb movements might be a fundamental mode of bilateral forelimb movements in rats, however, this idea needed to be investigated further.

The use of awake head-fixed rats under food restriction is less frequently reported than their use with water restriction, with the most recent report more than 10 years ago (Heck et al. 2007). Technical aspects of shaping behaviour by food reward may be a factor in the less frequent use of food restriction. The training of head-fixation in rats used graded exposure methods (Schwarz et al. 2010), based on compensating restraint anxiety with reward. In many experimental paradigms, water reward is easy to provide with a spout while animals remain restrained. In contrast, providing sold food items prompts rats to return from the restrainer by backward locomotion, making it difficult for the animal to associate the reward and environment. We, therefore, delivered jelly reward via stainless spout to guide rats to the head-fixed position, instead of providing pieces of solid food. In addition, a linear passive treadmill that we implemented significantly buffered backward locomotion reducing restraint stress on the animal. The two approaches synergistically improved training

efficiency.

Bimanual coordination deficits are observed in neurodegenerative disorders such as Parkinson's disease (Almeida et al. 2002; Johnson et al. 1998; Vercruysse et al. 2014), Huntington's disease (Brown et al. 1993; Johnson et al. 2000; Verbessem et al. 2002), Alzheimer's disease (Martin et al. 2017), and traumatic brain injury (Caeyenberghs et al. 2011; Gooijers et al. 2016). Parkinsonian patients have difficulty in asymmetric bimanual coordination (Almeida et al. 2002; Ponsen et al. 2006; Stelmach and Worringham 1988). Recent evidence suggests that recovery from hypokinesia in Parkinson's disease is not necessarily correlated with improvement in coordinated bimanual movements (Almeida and Brown 2013; Daneault et al. 2016; Igarashi et al. 2015). The decline in bimanual motor performance is also seen in healthy aging (Serbruyns et al. 2015). The unique mechanisms of bimanually coordinated movement need to be further studied to advance understanding of physiological mechanisms of neurodegenerative disorders and aging. We suggest that the presented measurement will illuminate bimanual coordination as a target of investigation by new – but almost exclusively rodent-based – research tools such as optogenetics, chemogenetics, *in vivo* electrophysiology, and multi-photon imaging.

ACKNOWLEDGEMENTS

We thank Dr. Sho Aoki for helpful discussions, and Dr. Andres Carrasco for comments on an earlier version of the manuscript.

GRANTS

This study was supported by Grant-in-Aid for JSPS Research Fellow Grant number 16J05329.

FIGURE LEGENDS

Fig. 1. Schematics of apparatus and imaging setup. (A) Illustration of the passive treadmill for the head-fixed behavioral device. Inset shows the assembled apparatus. (B and C) Schematic diagrams of the configuration of the rat positioned in the apparatus, from the front (B) and the side (C). The rat is shown on the passive treadmill holding a retrieved donut shaped food item. Two high-speed cameras are placed 45 cm below the transparent floor to monitor the reflective markers on the wrists. (D) View from camera 1 and camera 2 (inset). Note reflective markers attached to rat's wrists for semi-automatic tracing. (E) Timeline of the sequence of a trial of food handling and consumption.

Fig. 2. Egocentric coordinate reference frame in the recording frame, and segmentation of forelimb trajectory. (A-C) Forelimb position was projected on the egocentric coordinate system based on the reference marker. (A) Example of 3D printed reference frame of egocentric coordinates. Four triangularly placed reflective markers indicate the origin, posterior to anterior axis (P- A), left to right axis (L - R) and dorsal to ventral (D - V) axis of the rat (B). (C) Example of 3-D forelimb trajectories projected on the egocentric coordinate space. (D) Example 50 ms time window for data segmentation. Note the speed of the right and the left forelimb increased over time indicating bilateral movement initiation. (E) Representative segments of forelimb trajectories in each time window in (D). D, dorsal; V, ventral; A, anterior; P, posterior; R, right; L, left. Numbers in 3-D plots are expressed in millimeters.

Fig. 3. Decision tree for classification of segments.

Fig. 4. Representative behavior under head-fixed conditions. Frames in the left three columns show four different behaviors. Scatter plots in the right column illustrate corresponding 3-D forelimb trajectory. The color scale indicates the normalized time. Note that the duration of each behavior is variable. (A) Bimanual upward reach. Both forelimb simultaneously move toward the anterodorsal

side. (B) Bimanual downward reach. Both forelimb simultaneously move toward the posteroventral side. (C) Bimanual release. Both hand simultaneously release the food item and regrasp it to change the position of the hands. (D) Unimanual release. One hand release and regrasp of the food object with support of other hand. Abbreviations: D, dorsal; V, ventral; A, anterior; P, posterior; R, right; L, left. Numbers in 3-D plots are expressed in millimeters.

Fig. 5. Reconstruction of the whole sequence of forelimb movement during spontaneous food handling behavior. Positions of the right (blue) and the left (orange) forelimbs were captured by camera. Frames are shown rotated in 30° steps. Abbreviations: D, dorsal; V, ventral; A, anterior; P, posterior; R, right; L, left.

Fig. 6. Moving segments were exclusively selected by maximum speed function. (A) Probability distribution of speed of right and left forelimb movements across 5 rats. Left panel, linear scale. Reight panel, logarithmic scale. Note the dip of probability density at the threshold indicated by the dotted line (40 mm/sec). (B) Mean probability distribution of maximum speed function across 5 rats. (C) Mean proportion of moving segments in all segments. (D-E) Example trajectories of the segments in the resting state (D) and during movement (E). Abbreviations: D, dorsal; A, anterior; R, right; L, left. Numbers in 3-D plots are expressed in millimeters.

Fig. 7. Bilateral and unilateral forelimb movements during food handling. (A-C) Laterality of movement speed was quantified by speed ratio. (A) Graphical representation of speed ratio as a measure of laterality of left and right forelimb in speed. Each dot represents the mean speed of the right $\bar{V}_R$ and left forelimb $\bar{V}_L$ in a segment. The empty space at the left-bottom corner represents resting segments not included in the analysis. (B) Mean probability distribution of the speed ratio across 5 rats. (C-D) Example segments of bilateral and unilateral forelimb movements (C) and unimanual movements (D). Abbreviations: D, dorsal; A, anterior; R, right; L, left. Numbers in 3-D

plot are expressed in millimeters.

Fig. 8. Symmetric and asymmetry forelimb movements during food handling. (A-B) Asymmetry in movement direction was analyzed in terms of the error of movement vector direction between two forelimbs. (A) Graphical representation of mean angle of vector direction $\bar{\theta}$. Arrows indicates the example trajectory of left forelimb L and the mirrored right forelimb R_M. The asymmetry index $\bar{\theta}$ was calculated based on the error of movement vector direction between L and R_M. The dotted line illustrates the midline for the mirror transformation. (B) The probability distribution of the mean similarity of vector direction $\bar{\theta}$. (C-D) Examples of symmetric movement (C) and asymmetric movement (D). Abbreviations: D, dorsal; V, ventral; A, anterior; P, posterior; R, right; L, left. Numbers in 3-D plots are expressed in millimeters.

Fig. 9. Analytical pipeline enabling high-throughput of kinematic data for quantification of bilateral forelimb movements. (A) Pipeline of classification characterizes time course of behavioral states of spontaneous food handling behavior. The top two black traces indicate speed ratio and asymmetry indices respectively. The colored bars indicate the time of occurrence of each motor behavior defined by thresholding. The color code of each behavioral mode is shown in (B). Line graph indicates the speed of the right and left forelimb. (B) Magnified view of the shaded area in (A). (C) Corresponding actual trajectories of forelimbs. The color indicates the behavioral type shown in (B). Note that for clarity the color of unilateral movement overrides other categorizations when speed ratio exceeds the predefined threshold. (D) Quantitative analysis of behavioral types. Mean percentage of the behavioral type of movement classified in accordance with speed ratio (top) and asymmetry index (bottom). Abbreviations: Rest, resting; Bilat, bilateral forelimb movement; Unilat, unilateral forelimb movement; Sym, symmetric movement; Asym, asymmetric movement; D, dorsal; V, ventral; A, anterior; P, posterior; R, right; L, left.

REFERENCES

Allred RP, Adkins DL, Woodlee MT, Husbands LC, Maldonado MA, Kane JR, Schallert T, and Jones TA. The vermicelli handling test: a simple quantitative measure of dexterous forepaw function in rats. *J Neurosci Methods* 170: 229-244, 2008.

Almeida QJ, and Brown MJN. Is DOPA-Responsive Hypokinesia Responsible for Bimanual Coordination Deficits in Parkinson's Disease? *Front Neurol* 4: 89, 2013.

Almeida QJ, Wishart LR, and Lee TD. Bimanual coordination deficits with Parkinson's disease: the influence of movement speed and external cueing. *Mov Disord* 17: 30-37, 2002.

Azim E, Jiang J, Alstermark B, and Jessell TM. Skilled reaching relies on a V2a propriospinal internal copy circuit. *Nature* 508: 357-363, 2014.

Berman GJ, Choi DM, Bialek W, and Shaevitz JW. Mapping the stereotyped behaviour of freely moving fruit flies. *J R Soc Interface* 11: 2014.

Brown AR, and Teskey GC. Motor cortex is functionally organized as a set of spatially distinct representations for complex movements. *J Neurosci* 34: 13574-13585, 2014.

Brown RG, Jahanshahi M, and Marsden CD. The execution of bimanual movements in patients with Parkinson's, Huntington's and cerebellar disease. *J Neurol Neurosurg Psychiatry* 56: 295-297, 1993.

Burgos-Artizzu XP, Dollár P, Lin D, Anderson DJ, and Perona P. Social behavior recognition in continuous video. *IEEE Conference on Computer Vision and Pattern Recognition* 2012, p. 1322-1329.

Caeyenberghs K, Leemans A, Coxon J, Leunissen I, Drijkoningen D, Geurts M, Gooijers J, Michiels K, Sunaert S, and Swinnen SP. Bimanual coordination and corpus callosum microstructure in young adults with traumatic brain injury: a diffusion tensor imaging study. *Journal of neurotrauma* 28: 897-913, 2011.

Cardoso de Oliveira S, Gribova A, Donchin O, Bergman H, and Vaadia E. Neural interactions between motor cortical hemispheres during bimanual and unimanual arm movements. *The European journal of neuroscience* 14: 1881-1896, 2001.

Daneault JF, Carignan B, Sadikot AF, and Duval C. Subthalamic deep brain stimulation and dopaminergic medication in Parkinson's disease: Impact on inter-limb coupling. *Neuroscience* 335: 9-19, 2016.

Gooijers J, Beets IA, Albouy G, Beeckmans K, Michiels K, Sunaert S, and Swinnen SP. Movement preparation and execution: differential functional activation patterns after traumatic brain injury. *Brain* 139: 2469-2485, 2016.

Guo JZ, Graves AR, Guo WW, Zheng J, Lee A, Rodriguez-Gonzalez J, Li N, Macklin JJ, Phillips JW, Mensh BD, Branson K, and Hantman AW. Cortex commands the performance of skilled movement. *eLife* 4: e10774, 2015.

Hartley R, and Zisserman A. *Multiple View Geometry in Computer Vision*. Cambridge University Press, 2003.

Heck DH, Thach WT, and Keating JG. On-beam synchrony in the cerebellum as the mechanism for the timing and coordination of movement. *Proc Natl Acad Sci U S A* 104: 7658-7663, 2007.

Hira R, Ohkubo F, Ozawa K, Isomura Y, Kitamura K, Kano M, Kasai H, and Matsuzaki M.

Spatiotemporal dynamics of functional clusters of neurons in the mouse motor cortex during a voluntary movement. *J Neurosci* 33: 1377-1390, 2013.

Igarashi M, Habata T, Akita H, Noda K, Ogata M, and Saji M. The NR2B antagonist, ifenprodil, corrects the L-DOPA-induced deficit of bilateral movement and reduces c-Fos expression in the subthalamic nucleus of hemiparkinsonian rats. *Neurosci Res* 96: 45-53, 2015.

Isomura Y, Harukuni R, Takekawa T, Aizawa H, and Fukai T. Microcircuitry coordination of cortical motor information in self-initiation of voluntary movements. *Nat Neurosci* 12: 1586-1593, 2009.

Johnson KA, Bennett JE, Georgiou N, Bradshaw JL, Chiu E, Cunnington R, and Iansek R. Bimanual coordination in Huntington's disease. *Exp Brain Res* 134: 483-489, 2000.

Johnson KA, Cunnington R, Bradshaw JL, Phillips JG, Iansek R, and Rogers MA. Bimanual coordination in Parkinson's disease. *Brain* 121: 743-753, 1998.

Kawai R, Markman T, Poddar R, Ko R, Fantana AL, Dhawale AK, Kampff AR, and Ölveczky BP. Motor Cortex Is Required for Learning but Not for Executing a Motor Skill. *Neuron* 86: 800-812, 2015.

Liu J, Jiebo L, and Shah M. Recognizing realistic actions from videos "in the wild". *IEEE Conference on Computer Vision and Pattern Recognition* 2009, p. 1996-2003.

Manfré G, Clemensson EKH, Kyriakou EI, Clemensson LE, van der Harst JE, Homberg JR, and Nguyen HP. The BACHD Rat Model of Huntington Disease Shows Specific Deficits in a Test Battery of Motor Function. *Front Behav Neurosci* 11: 2017.

Martin E, Blais M, Albaret J-M, Pariente J, and Tallet J. Alteration of rhythmic unimanual tapping and anti-phase bimanual coordination in Alzheimer's disease: A sign of inter-hemispheric disconnection? *Hum Mov Sci* 55: 43-53, 2017.

Ollerenshaw DR, Bari BA, Millard DC, Orr LE, Wang Q, and Stanley GB. Detection of tactile inputs in the rat vibrissa pathway. *J Neurophysiol* 108: 479-490, 2012.

Palmér T, Tamtè M, Halje P, Enqvist O, and Petersson P. A system for automated tracking of motor components in neurophysiological research. *J Neurosci Methods* 205: 334-344, 2012.

Panigrahi B, Martin KA, Li Y, Graves AR, Vollmer A, Olson L, Mensh BD, Karpova AY, and Dudman JT. Dopamine Is Required for the Neural Representation and Control of Movement Vigor. *Cell* 162: 1418-1430, 2015.

Ponsen MM, Daffertshofer A, van den Heuvel E, Wolters E, Beek PJ, and Berendse HW. Bimanual coordination dysfunction in early, untreated Parkinson's disease. *Parkinsonism Relat Disord* 12: 246-252, 2006.

Reinkensmeyer DJ, Burdet E, Casadio M, Krakauer JW, Kwakkel G, Lang CE, Swinnen SP, Ward NS, and Schweighofer N. Computational neurorehabilitation: modeling plasticity and learning to predict recovery. *J Neuroeng Rehabil* 13: 42, 2016.

Robie AA, Seagraves KM, Egnor SER, and Branson K. Machine vision methods for analyzing social interactions. *J Exp Biol* 220: 25-34, 2017.

Schwarz C, Hentschke H, Butovas S, Haiss F, Stüttgen MC, Gerdjikov TV, Bergner CG, and Waiblinger C. The Head-fixed Behaving Rat—Procedures and Pitfalls. *Somatosens Mot Res* 27: 131-148, 2010.

Serbruyns L, Gooijers J, Caeyenberghs K, Meesen RL, Cuypers K, Sisti HM, Leemans A, and Swinnen SP. Bimanual motor deficits in older adults predicted by diffusion tensor imaging metrics of corpus callosum subregions. *Brain Struct Funct* 220: 273-290, 2015.

Stelmach GE, and Worringham CJ. The control of bimanual aiming movements in Parkinson's disease. *J Neurol Neurosurg Psychiatry* 51: 223-231, 1988.

Swinnen SP. Intermanual coordination: from behavioural principles to neural-network interactions. *Nat Rev Neurosci* 3: 348-359, 2002.

Swinnen SP, Dounskaia N, Levin O, and Duysens J. Constraints during bimanual coordination: the role of direction in relation to amplitude and force requirements. *Behav Brain Res* 123: 201-218, 2001.

Swinnen SP, Jardin K, Verschueren S, Meulenbroek R, Franz L, Dounskaia N, and Walter CB. Exploring interlimb constraints during bimanual graphic performance: effects of muscle grouping and direction. *Behav Brain Res* 90: 79-87, 1998.

Swinnen SP, and Wenderoth N. Two hands, one brain: cognitive neuroscience of bimanual skill. *Trends Cogn Sci* 8: 18-25, 2004.

Tennant KA, Asay AL, Allred RP, Ozburn AR, Kleim JA, and Jones TA. The vermicelli and capellini handling tests: simple quantitative measures of dexterous forepaw function in rats and mice. *J Vis Exp* e2076, 2010.

van Delden AL, Peper CL, Kwakkel G, and Beek PJ. A systematic review of bilateral upper limb training devices for poststroke rehabilitation. *Stroke Res Treat* 2012: 972069, 2012.

Verbessem P, Op't Eijnde B, Swinnen S, Vangheluwe S, Hespel P, and Dom R. Unimanual and bimanual voluntary movement in Huntington's disease. *Exp Brain Res* 147: 529-537, 2002.

Vercruysse S, Spildooren J, Heremans E, Wenderoth N, Swinnen SP, Vandenberghe W, and Nieuwboer A. The neural correlates of upper limb motor blocks in Parkinson's disease and their relation to freezing of gait. *Cereb Cortex* 24: 3154-3166, 2014.

Wang X, Liu Y, Li X, Zhang Z, Yang H, Zhang Y, Williams PR, Alwahab NSA, Kapur K, Yu B, Zhang Y, Chen M, Ding H, Gerfen CR, Wang KH, and He Z. Deconstruction of Corticospinal Circuits for Goal-Directed Motor Skills. *Cell* 171: 440-455, 2017.

Whishaw IQ, and Coles BL. Varieties of paw and digit movement during spontaneous food handling in rats: postures, bimanual coordination, preferences, and the effect of forelimb cortex lesions. *Behav Brain Res* 77: 135-148, 1996.

Whishaw IQ, Faraji J, Kuntz J, Mirza Agha B, Patel M, Metz GAS, and Mohajerani MH. Organization of the reach and grasp in head-fixed vs freely-moving mice provides support for multiple motor channel theory of neocortical organization. *Exp Brain Res* 235: 1919-1932, 2017a.

Whishaw IQ, Faraji J, Kuntz JR, Mirza Agha B, Metz GAS, and Mohajerani MH. The syntactic organization of pasta-eating and the structure of reach movements in the head-fixed mouse. *Sci Rep* 7: 10987, 2017b.

Wu T, Wang L, Hallett M, Li K, and Chan P. Neural correlates of bimanual anti-phase and in-phase movements in Parkinson's disease. *Brain* 133: 2394-2409, 2010.

643 **Xu T, Yu X, Perlik AJ, Tobin WF, Zweig JA, Tennant K, Jones T, and Zuo Y**. Rapid formation and selective
644 stabilization of synapses for enduring motor memories. *Nature* 462: 915-919, 2009.

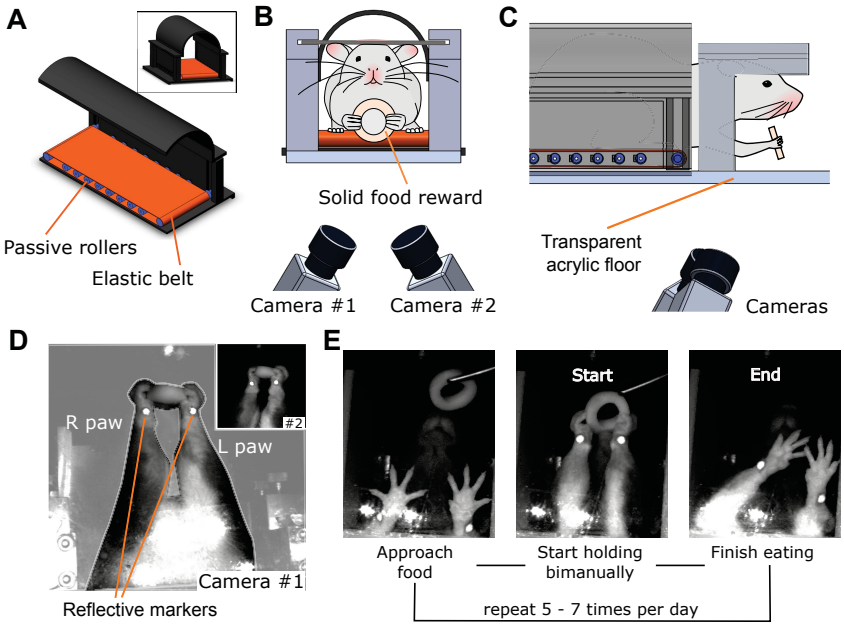
A
B
C
Passive rollers
Elastic belt
Solid food reward
Camera #1
Camera #2
Transparent
acrylic floor
Cameras
D
E
R paw
L paw
#2
Camera #1
Reflective markers
Start
End
Approach
food
Start holding
bimanually
Finish eating
repeat 5 - 7 times per day

Figure 1

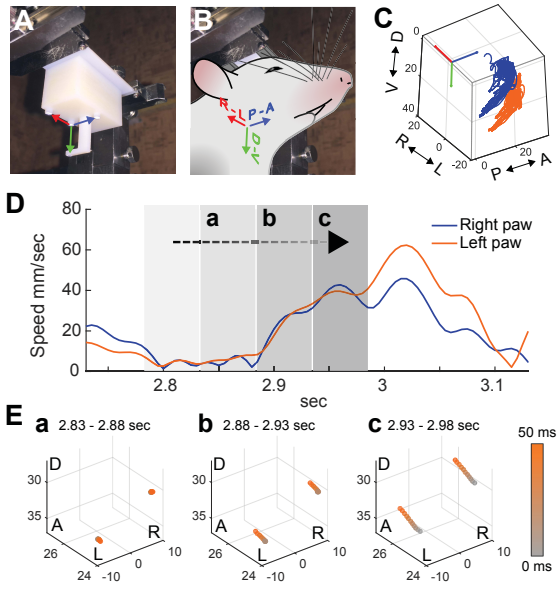
A
B
C
D
E
Speed mm/sec
sec
Right paw
Left paw
a
b
c
2.83 - 2.88 sec
2.88 - 2.93 sec
2.93 - 2.98 sec
50 ms
0 ms

Figure 2

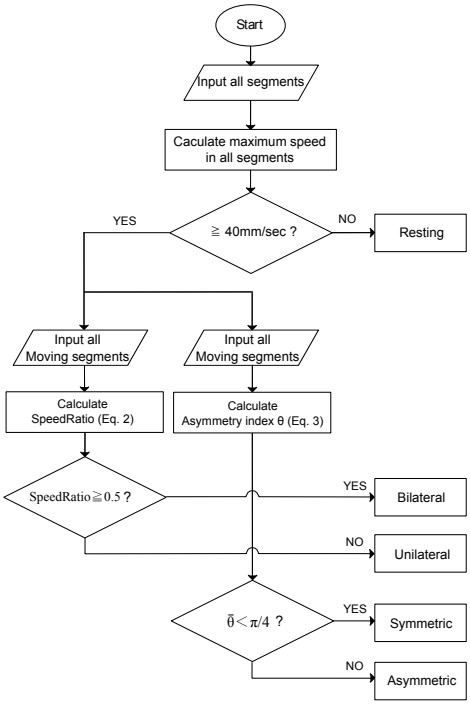
Start
Input all segments
Caculate maximum speed in all segments
YES
≧ 40mm/sec ?
NO
Resting
Input all Moving segments
Input all Moving segments
Calculate SpeedRatio (Eq. 2)
Calculate Asymmetry index θ (Eq. 3)
SpeedRatio≧0.5 ?
YES
Bilateral
NO
Unilateral
θ̃<π/4 ?
YES
Symmetric
NO
Asymmetric

Figure 3

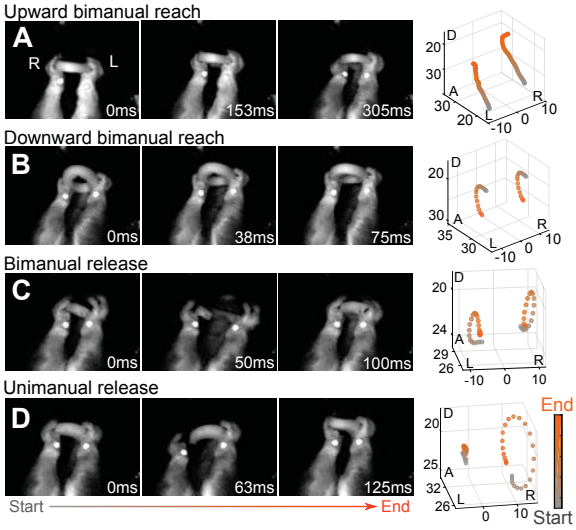
Upward bimanual reach
A
R
L
0ms
153ms
305ms
Downward bimanual reach
B
0ms
38ms
75ms
Bimanual release
C
0ms
50ms
100ms
Unimanual release
D
0ms
63ms
125ms
Start
End
D
A
L
R
End
Start

Figure 4

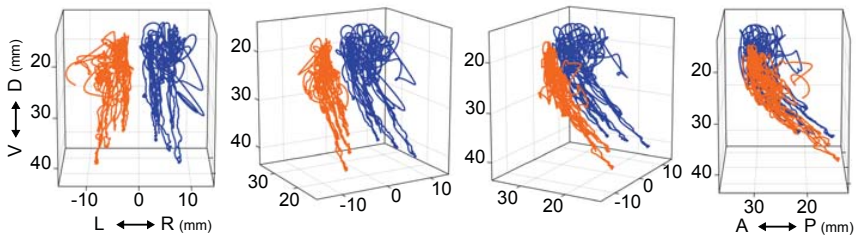
V
D (mm)
20
30
40
-10
0
10
L
R (mm)
20
30
40
30
20
-10
0
10
20
30
40
30
20
-10
0
10
20
30
40
30
20
A
P (mm)

Figure 5

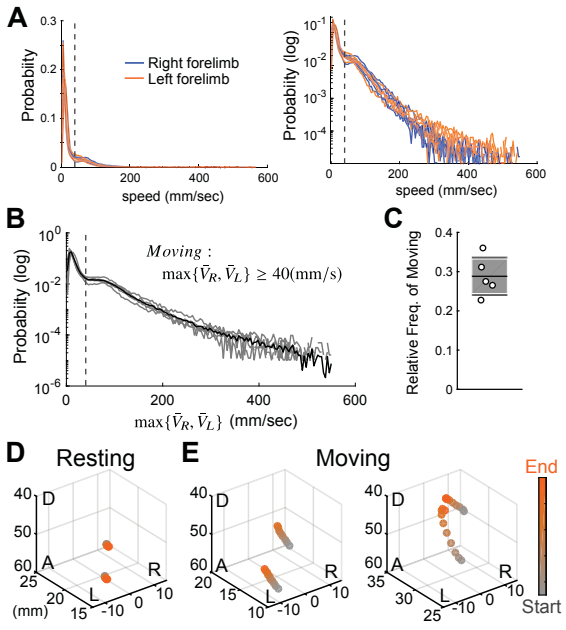
A
Probability
Right forelimb
Left forelimb
speed (mm/sec)
Probability (log)
speed (mm/sec)
B
Probability (log)
Moving :
max{$\bar{V}_R, \bar{V}_L$} ≥ 40(mm/s)
max{$\bar{V}_R, \bar{V}_L$} (mm/sec)
C
Relative Freq. of Moving
D
Resting
E
Moving
End
Start
(mm)

Figure 6

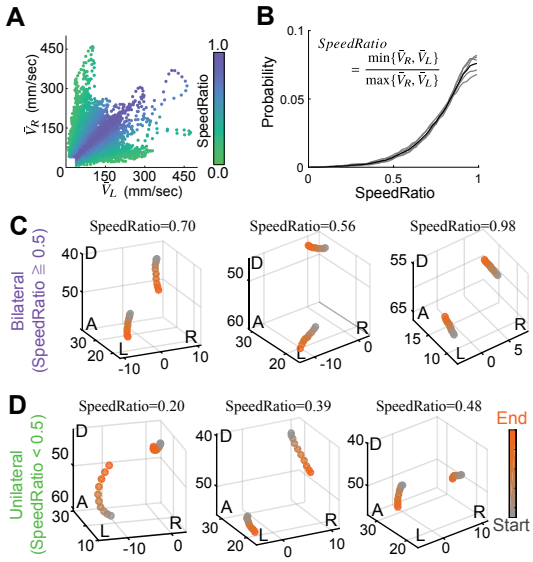
A
B
C
D
SpeedRatio
Probability
SpeedRatio=0.70
SpeedRatio=0.56
SpeedRatio=0.98
SpeedRatio=0.20
SpeedRatio=0.39
SpeedRatio=0.48
Bilateral
(SpeedRatio ≥ 0.5)
Unilateral
(SpeedRatio < 0.5)
End
Start

Figure 7

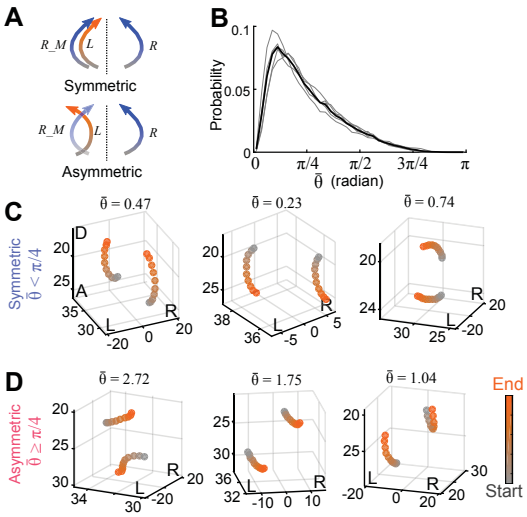
A
R_M
L
R
Symmetric
R_M
L
R
Asymmetric
B
Probability
0.1
0.05
0
0
π/4
π/2
3π/4
π
θ̄ (radian)
C
Symmetric
θ̄ < π/4
θ̄ = 0.47
θ̄ = 0.23
θ̄ = 0.74
D
A
L
R
D
Asymmetric
θ̄ ≥ π/4
θ̄ = 2.72
θ̄ = 1.75
θ̄ = 1.04
End
Start

Figure 8

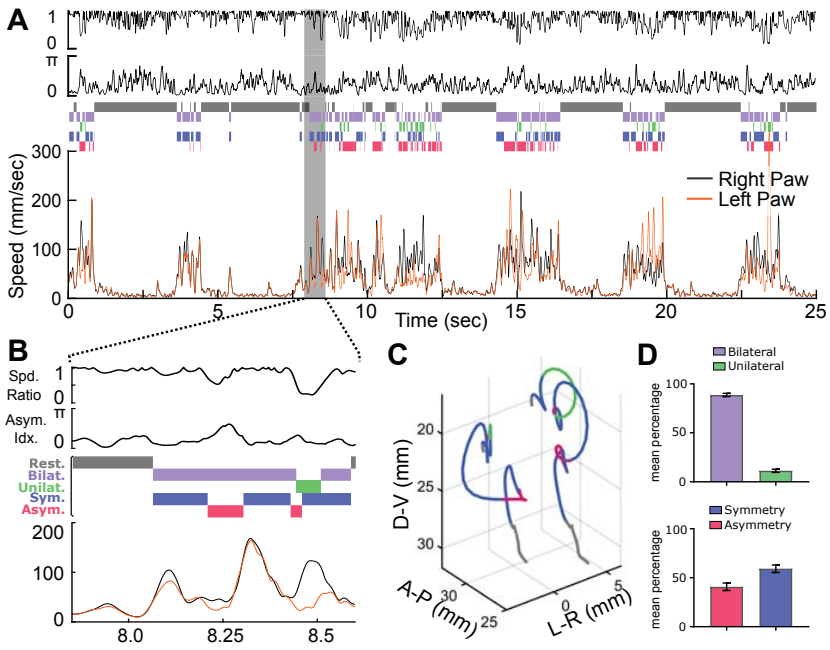
A
1
0
π
0
300
200
100
0
Speed (mm/sec)
Right Paw
Left Paw
0
5
10
15
20
25
Time (sec)
B
Spd. Ratio
Asym. Idx.
Rest.
Bilat.
Unilat.
Sym.
Asym.
200
100
0
8.0
8.25
8.5
C
D-V (mm)
20
25
30
A-P (mm)
30
25
0
5
L-R (mm)
D
Bilateral
Unilateral
mean percentage
100
50
0
Symmetry
Asymmetry
mean percentage
100
50
0